ACS APPLIED MATERIALS & INTERFACES

Research Article

www.acsami.org

Anomalous Interfacial Lithium Storage in Graphene/TiO_2 for Lithium Ion Batteries

Enzuo Liu,*[,†,‡] Jiamei Wang,[†] Chunsheng Shi,[†] Naiqin Zhao,*[,†,‡] Chunnian He,[†] Jiajun Li,[†] and Jian-Zhong Jiang[§]

[†]School of Materials Science and Engineering and Tianjin Key Laboratory of Composites and Functional Materials, Tianjin University, Tianjin 300072, China

[‡]Collaborative Innovation Center of Chemical Science and Engineering, Tianjin 300072, China

[§]International Center for New-Structured Materials (ICNSM), Laboratory of New-Structured Materials, State Key Laboratory of Silicon Materials, and Department of Materials Science and Engineering, Zhejiang University, Hangzhou, 310027, China

Supporting Information

ABSTRACT: Graphene/metal-oxide nanocomposites have been widely studied as anode materials for lithium ion batteries and exhibit much higher lithium storage capacity beyond their theoretical capacity through mechanisms that are still poorly understood. In this research, we present a comprehensive understanding in microscale of the discharge process of graphene/TiO_2 containing surface, bulk, and interfacial lithium storage based on the first-principles total energy calculations. It is revealed that interfacial oxygen atoms play an important role on the interfacial lithium storage. The additional capacity originating from surface and interfacial lithium storage via an electrostatic capacitive mechanism contributes significantly to the electrode capacity. The research demonstrates that for nanocomposites used in energy storage materials, electrode and capacitor behavior could be optimized to develop high-performance electrode materials with the balance of storage capacity and rate.

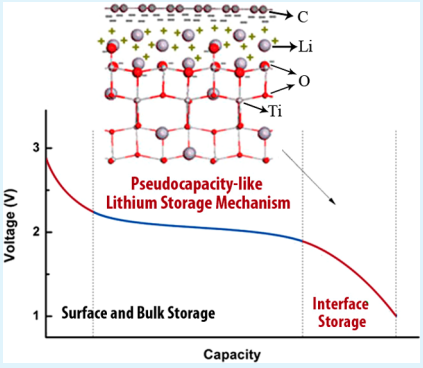

KEYWORDS: *interfacial lithium storage, pseudocapacity-like storage mechanism, interfacial oxygen atoms, discharge process, first-principles calculations*

1. INTRODUCTION

Lithium ion batteries with high power and energy densities are required due to the development of mobile electronics and electric vehicles. Exploiting electrode materials with long cycle life, high capacity, and fast charging/discharging rates is one of the main challenges. Metal oxides, such as Fe_2O_3, SnO_2, TiO_2, etc., have been widely researched as anode materials for Li ion batteries.[1] However, metal oxides exhibit poor cycling stability due to the large volume swing generated during the charge−discharge process and poor rate performance because of their low electrical conductivity. Graphene addition is widely used to improve the structure stability and rate performance of the metal oxide, since the volume swing during the charging/discharging processes can be alleviated by the porous structure of the composites and the electrical conductivity is expected to be enhanced by the graphene layer within the metal oxide nanomaterials.[2] Very recently, experimental results reveal that the graphene-modified electrode materials exhibit lithium capacity beyond theoretical capacity.[3,4] Reduced graphene oxide exhibits considerable lithium storage capacity.[5] Therefore, for the graphene/metal oxide nanocomposites, there may be a synergetic effect of graphene and metal oxide resulting in the additional lithium storage capacity. Moreover, for metal oxides the additional capacity is attributed to surface lithium storage via the decomposition of LiOH into Li_2O and LiH.[6] Thus, for graphene/metal oxide nanocomposites, Li ion storage behavior at the interface of graphene/metal oxide is expected to be different from that in bulk metal oxide, as well as that at pure metal oxide surfaces. It is very important to study the interfacial Li ion storage behavior between graphene and metal oxides in microscale, as well as the effect of graphene on the electronic structure of the electrode materials, in order to understand the additional capacity in graphene/metal oxide.

In this research, we systematically investigate the Li ion storage behavior in the graphene-nanoribbon (GNR) modified anatase TiO_2 which has high structure stability and stable performance during lithium insertion/extraction as an anode for Li ion batteries.[7,8] It is revealed that interfacial oxygen atoms as the bridge of GNR and TiO_2 play an important role in the Li ion storage behavior at the interface, and during Li insertion, the bond between interfacial oxygen and carbon atoms in GNR is broken, which acts as to reduce GNR and enhances the electrical conductivity of the system. A pseudocapacitive interfacial Li ion storage mechanism is proposed based on

Received: July 30, 2014
Accepted: September 23, 2014
Published: September 23, 2014

   dx.doi.org/10.1021/am5050423 | ACS Appl. Mater. Interfaces 2014, 6, 18147−18151

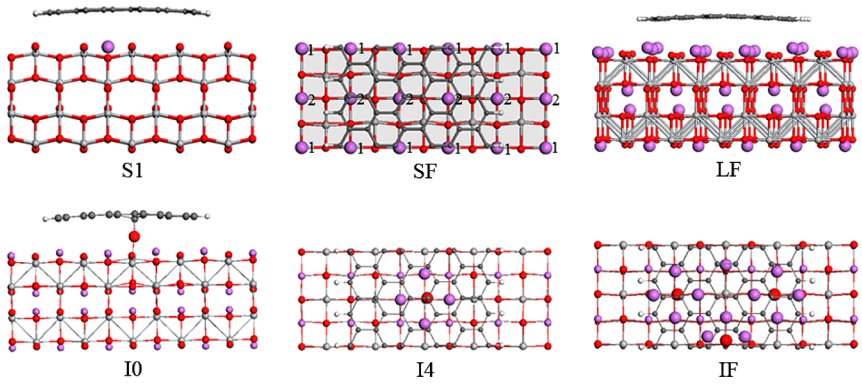

Figure 1. Atomic configurations with different lithium content in GNR-modified TiO_2 (001) surface. Side view of S1, LF, I0, and top view of SF, I4, IF are presented. The red, light gray, gray, purple, and white balls indicate O, Ti, C, Li, and H atoms, respectively. Larger red and purple balls in I0, I4, and IF indicate interfacial oxygen and lithium atoms, respectively.

the electronic structure analysis. Through detailed research on the Li ion insertion process, a discharge process model is illustrated in microscale which reproduces the experimental discharge curve of graphene-modified TiO_2 ultrathin nanosheets well.

2. COMPUTATIONAL METHODS

The projector augmented wave (PAW) formalism of density functional theory as implemented in the Vienna ab initio Simulation Package (VASP)[9−12] is used in the system energy and electronic structure calculations. The exchange-correlation functional is approximated with the local density approximation. The generalized gradient approximation proposed by Perdew, Burke, and Ernzerhof (PBE),[13] and DFT $+U$[14,15] is adopted in order to confirm the calculation results (see the Supporting Information). The Gaussian smearing method[16] was used, and the width of smearing was chosen as 0.05 eV. The energy cutoff for plane-wave expansion of the PAW's is 500 eV. TiO_2 (001) is selected as the research object for the good electrochemical performance of graphene/anatase TiO_2 nanosheets with exposed {001} facets.[17] As shown in Figure 1, for TiO_2 (001) and $Li_{0.5}TiO_2$ (001) surfaces with GNR adsorbed, a 2 × 5 supercell containing 80 O and 40 Ti atoms is used. $Li_{0.5}TiO_2$ with orthorhombic titanate phase[18] is adopted. In the c direction, four TiO_2 layers are used with the bottom TiO_2 layer fixed. For geometry optimizations, all the other internal coordinates are relaxed until the Hellmann−Feynman forces are less than 0.03 eV/Å. The Brillouin zone is sampled using Monkhorst−Pack scheme[19] with 3 × 1 × 1 k-point grid. GNR containing 36 C and 6 H atoms is adsorbed on TiO_2 (001) surface. The lattice of GNR is elongated 2.2% to match the surface lattice of TiO_2. The binding energy of Li is defined as $E_b = -(E_T - E_0 - nE_{Li})/n$, where E_0 is the energy of the studied system, E_T is the energy of the corresponding system with n Li atoms adsorbed, and E_{Li} is the energy of one Li atom in bcc bulk.

3. RESULTS AND DISCUSSION

When one Li atom is adsorbed at the first surface layer of TiO_2 (001) surface with GNR modified, the most stable adsorption site is in between the surface O atoms (S1 in Figure 1), and the binding energy is 2.88 eV which is much larger than that (2.16 eV) of one Li insertion in the TiO_2 bulk (see the Supporting Information, TiO_2 in Figure S1). The configuration with the surface adsorption sites half occupied (sites 1 in SF) has been studied, and the adsorption energy is 2.56 eV, still larger than that of one Li insertion in TiO_2 bulk. For the Li atoms further occupation of the other half of the surface adsorption sites (sites 2 in SF), the binding energy is 1.91 eV, only slightly larger than the average binding energy of Li atom in $Li_{0.5}TiO_2$ bulk (1.90 eV, $Li_{0.5}TiO_2$ in Figure S1). It should be pointed out that the Li content in the surface TiO_2 layer is twice larger than Li content in each TiO_2 layer of $Li_{0.5}TiO_2$ bulk. Thus, surface Li storage contributes to the addition storage capacity.

Subsequently, we investigate the configuration of $Li_{0.5}TiO_2$ (001) surface with all the surface adsorption site occupied (LF in Figure 1, in total 15 Li adsorption sites below the first surface layer). We find that the average binding energy of all the subsurface Li atoms is 2.06 eV, which is larger than the average binding energy of Li atom in $Li_{0.5}TiO_2$ bulk (1.90 eV, $Li_{0.5}TiO_2$ in Figure S1) due to the existence of Li atoms inserted in the subsurface layers and the fixed bottom layer of the supercell whose coordination environment is different from that of Li atoms in $Li_{0.5}TiO_2$ bulk. To prove this assumption, one Li atom adsorption at subsurface layer of TiO_2 (001) (GR/TiO_2 (001) in Figure S1) has been calculated and the binding energy is 2.28 eV, which is slightly larger than that of one Li atom inserted (2.16 eV) in TiO_2 bulk.

Based on the binding energies of Li atoms in different configurations, it could be expected that in the Li insertion process, Li atoms first occupy partial surface adsorption sites in between surface O atoms with high binding energy, and then occupy subsurface insertion sites and the bulk insertion sites in the solid-solution manner with low Li content,[20] accompanying with the drastic decrease of the discharge voltage consistent with the experimental result.[17] Moreover, the binding energy of Li atom in S1 (2.88 eV) is much larger than that (2.31 eV) of the Li adsorption on TiO_2 (001) surface with 1 × 4 reconstruction (TiO_2 (001) in Figure S1). As shown in Figure 2a, Li insertion at surface results in electron accumulation near graphene and covalent-like bonding between Li and surface O atoms, which enhance the binding energy of Li at surface in GNR-modified TiO_2 (001).

More additional Li atoms may adsorb at the interface between GNR and TiO_2 (001) surface. Two configurations for one and six additional Li atoms inserted at the interface are considered (Figure S2), and the binding energies are −0.30 and 0.11 eV, respectively. Due to the high voltage in the experimental electrochemical tests,[17] the additional Li atoms cannot account for the storage capacity. On the other hand, Ti−O−C bonds forms between TiO_2 nanosheet and reduced

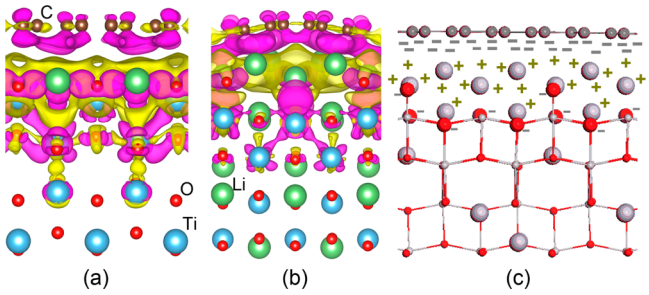

Figure 2. Electronic density differences of configurations LF (a) and IF (b) in Figure 1, which are obtained by subtracting electronic densities of Li atoms adsorbed at surface or interface and configurations LF and IF without Li atoms insertion at surface or interface from that of LF and IF. The electronic density is plotted via VESTA.[23] The isosurface contours correspond to 1.5×10^{-3} and 2.5×10^{-3} e/Å^3 for a and b, respectively. Purple and yellow colors indicate the positive and negative electronic density, respectively. (c) Schematic model for the explanation of interfacial-storage mechanism.

graphene oxide,[21] and interfacial bridge oxygen atoms have also been revealed between NiO and graphene.[22] Thus, configuration I0 in Figure 1 with interfacial oxygen atoms between GNR and TiO_2 (001) is considered. The average binding energies with 1, 2, and 4 Li atoms adsorbed around the interfacial oxygen atom are 1.56, 1.46, and 1.17 eV, respectively. The configuration with four Li atoms adsorbed around the interfacial oxygen atom is shown as I4 in Figure 1, and the interfacial Li atoms are adsorbed above oxygen atoms in the surface TiO_2 layer. Furthermore, we investigate the configuration with three interfacial oxygen atoms and all the sites above oxygen atom in the surface TiO_2 layer between the GNR and TiO_2 (001) occupied (configuration IF in Figure 1, totally 12 interfacial Li atoms). The average binding energy of the interfacial Li atoms is 1.01 eV. Thus, the interfacial Li storage behavior of GNR/TiO_2 composites is significantly enhanced by the interfacial oxygen atoms. Moreover, it is found that with the insertion of Li atoms at interface, the bond between O and C atoms in GNR is broken, which could serve as the reduction process of graphene oxide, and the electrical conductivity of the system is expected to be enhanced. As shown in Figure 3, with the Li atom insertion in the interface, the electronic density of states around Fermi energy is gradually increased. Thus, graphene oxide or reduced graphene oxide used in the fabrication of graphene/metal oxide composites could better serve as the conductor with Li insertion at interface.

As shown in Figure 2a, the introduction of surface Li atoms causes an electronic charge transfer toward GNR. Surface O atoms bond with Li atoms via valence-like bond and serve as host for Li^+, while GNR serves as electron acceptor. Thus, a charge separation forms. With the interfacial Li atoms insertion, an additional electronic charge transfers toward the GNR (Figure 2b). The interfacial bridge O atoms serve as host for Li^+ via ionic bonding with Li atoms. Thus, the anomaly interfacial storage mechanism can be shown in Figure 2c, which is pseudocapacity-like with charge separation. In nanocomposites for energy storage, both capacitor behavior and electrode behavior contribute to the energy storage capacity. Through carefully control the interface structure and composition, an optimization of storage capacity versus rate is expected to be obtained. Recently experimental results also confirm the contribution of pseudocapacity to fast lithium storage in metal oxide nanomaterials.[24,25]

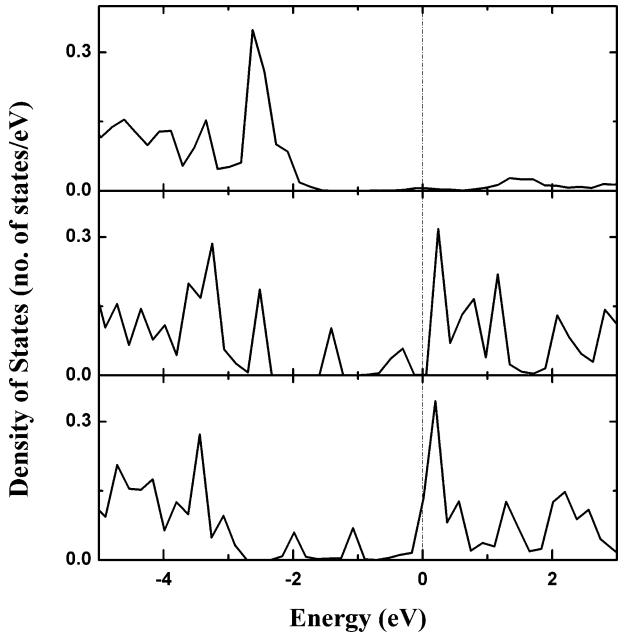

Figure 3. Density of 2p states of the C atom bonding with the interfacial oxygen atoms in configuration I0 in Figure 1 (top) and the corresponding C atoms in configuration I4 (middle) and IF (bottom). The Fermi energy is set as 0 eV.

Based on above discussion, the discharging process (Figure 4a) of graphene-modified TiO_2 ultrathin nanosheet (Figure 4b)

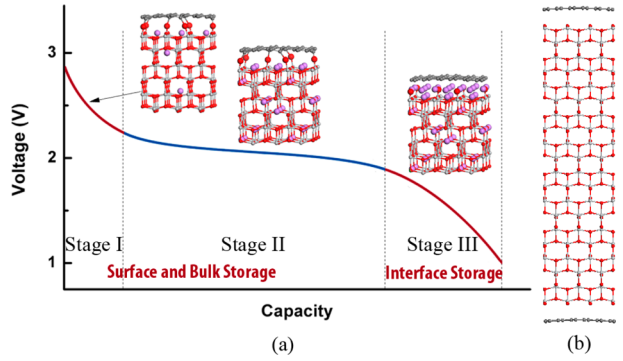

Figure 4. Schematic illustration of the discharge process (a) of graphene-modified TiO_2 ultrathin nanosheet (b). The sketch shows atomic structures at different discharge stages.

could be schematically illustrated. First, Li atom will occupy TiO_2 surface sites, subsurface adsorption site and the bulk insertion site in the solid-solution manner with low Li content (stage I). Second, Li atoms gradually insert into TiO_2 bulk, and anatase TiO_2 changes into $Li_{0.5}TiO_2$ with titanate phase, as well as the full occupation of surface adsorption sites. Surface and bulk storage constitute stages I and II. Third, Li atoms insert at the interface sites via interfacial oxygen atoms (interface storage, stage III). Thus, surface and bulk storage contribute to the monotonous potential drop and the potential plateau, while interface storage contributes to the slope potential drop in the discharging process of the graphene/TiO_2 electrode. Surface and interfacial lithium storage provides additional capacity beyond the theoretical capacity of 167.5 mAh g^{-1} with lithium ions occupying about half of the available interstitial octahedral sites in TiO_2.

dx.doi.org/10.1021/am5050423 | ACS Appl. Mater. Interfaces 2014, 6, 18147−18151

If we suppose that the TiO_2 nanosheet is 4.5 nm thick with both surfaces covered by graphene with 20 at% oxygen content (Figure 4b) and that Li atoms at the interface occupy all the sites above oxygen atoms of the first surface layer (configurations inserted in Figure 4a), the capacity of the system is expected to be 226 mAh/g, with the contribution of surface, bulk, and interface storage about 13%, 60%, and 27%, respectively. The capacity is well reproduced in the experimental results reported.[17] About 35% additional Li storage capacity beyond the TiO_2 theoretical capacity is from the surface and interface storage process via a pseudocapacity-like energy storage mechanism.

4. CONCLUSIONS

In conclusion, Li atom adsorption at the TiO_2 (001) surface is significantly enhanced due to GNR modification. Li adsorption at the GNR/TiO_2 (001) interface is around interfacial oxygen atoms, and with Li adsorption at the interface, the reduction process of graphene oxide benefits electrical conductivity. During the surface and interface storage process, surface and interfacial O atoms serve as hosts for Li^+ and bond with Li atoms via valence-like and ionic bonds, respectively, while GNR serves as an electron acceptor, resulting in a charge separation. Surface and interface storage processes contribute to additional Li storage capacity beyond the theoretical capacity via an interfacial pseudocapacity-like storage mechanism. The discharge process of graphene-modified TiO_2 can be divided into surface, bulk, and interface storage, with surface and bulk storage contributing to the monotonous potential drop and potential plateau and interface storage contributing to the slope potential drop in the discharge curve. The research results present a comprehensive understanding (in microscale) of the discharge process of graphene/metal oxide and indicate the possibility of the development of electrode materials with high capacity and fast charging/discharging rates through an interfacial storage mechanism in graphene/metal oxide nanocomposite electrodes.

■ ASSOCIATED CONTENT

Supporting Information

Different structures used for the test to determine the stable Li adsorption sites in GNR/TiO_2 (001) and the calculations results obtained using GGA and DFT +*U* approximation. This material is available free of charge via the Internet at http://pubs.acs.org.

■ AUTHOR INFORMATION

Corresponding Authors

*E-mail: ezliu@tju.edu.cn (E.L.)
*E-mail: nqzhao@tju.edu.cn (N.Z.).

Notes

The authors declare no competing financial interest.

■ ACKNOWLEDGMENTS

Calculations were carried out at the Shanghai Supercomputer Center. This work was supported by the National Natural Science Foundation of China (Grants No. 11474216, 51272173, and 51371157), China-EU Science and Technology Cooperation Project (No. 1206), the National Key Basic Research Program of China (2012CB825700), the key technologies R & D program of Tianjin (12ZCZDGX00800), and the Innovation Foundation of Tianjin University.

■ REFERENCES

(1) Wang, Z.; Zhou, L.; David Lou, X. W. Metal Oxide Hollow Nanostructures for Lithium Ion Batteries. *Adv. Mater. (Weinheim, Ger.)* **2012**, *24*, 1903−1911.
(2) Han, S.; Wu, D.; Li, S.; Zhang, F.; Feng, X. Graphene: a Two-Dimensional Platform for Lithium Storage. *Small* **2013**, *9*, 1173−1187.
(3) Zhu, J.; Yang, D.; Rui, X.; Sim, D.; Yu, H.; Hng, H. H.; Hoster, H. E.; Ajayan, P. M.; Yan, Q. Facile Preparation of Ordered Porous Graphene-Metal Oxide@C Binder-Free Electrodes with High Li Storage Performance. *Small* **2013**, *9*, 3390−3397.
(4) Hu, L.-H.; Wu, F.-Y.; Lin, C.-T.; Khlobystov, A. N.; Li, L.-J. Graphene-Modified $LiFePO_4$ Cathode for Lithium Ion Battery Beyond Theoretical Capacity. *Nat. Commun.* **2013**, *4*, 1687.
(5) Ha, S. H.; Jeong, Y. S.; Lee, Y. J. Free Standing Reduced Graphene Oxide Film Cathodes for Lithium Ion Batteries. *ACS Appl. Mater. Interfaces* **2013**, *5*, 12295−12303.
(6) Hu, Y.-Y.; Liu, Z.; Nam, K.-W.; Borkiewicz, O. J.; Cheng, J.; Hua, X.; Dunstan, M. T.; Yu, X.; Wiaderek, K. M.; Du, L.-S.; Chapman, K. W.; Chupas, P. J.; Yang, X.-Q.; Grey, C. P. Origin of Additional Capacities in Metal Oxide Lithium-ion Battery Electrodes. *Nat. Mater.* **2013**, *12*, 1130−1136.
(7) Xin, X.; Zhou, X.; Wu, J.; Yao, X.; Liu, Z. Scalable Synthesis of TiO_2/Graphene Nanostructured Composite with High-Rate Performance for Lithium Ion Batteries. *ACS Nano* **2012**, *6*, 11035−11043.
(8) Yang, S.; Feng, X.; Mullen, K. Sandwich-Like, Graphene-Based Titania Nanosheets with High Surface Area for Fast Lithium Storage. *Adv. Mater. (Weinheim, Ger.)* **2011**, *23*, 3575−3579.
(9) Kresse, G.; Hafner, J. *Ab Initio* Molecular Dynamics for Liquid Metals. *Phys. Rev. B: Condens. Matter Mater. Phys.* **1993**, *47*, 558−561.
(10) Kresse, G.; Furthmüller, J. Efficiency of Ab-Initio Total Energy Calculations for Metal and Semiconductors Using a Plane-Wave Basis Set. *Comput. Mater. Sci.* **1996**, *6*, 15−50.
(11) Kresse, G.; Furthmüller, J. Efficient Iterative Schemes for Ab Initio Total-Energy Calculations Using a Plane-Wave Basis Set. *Phys. Rev. B: Condens. Matter Mater. Phys.* **1996**, *54*, 11169−11186.
(12) Kresse, G.; Joubert, D. From Ultrasoft Pseudopotentials to the Projector Augmented Wave Method. *Phys. Rev. B: Condens. Matter Mater. Phys.* **1999**, *59*, 1758−1775.
(13) Perdew, J. P.; Burke, K.; Ernzerhof, M. Generalized Gradient Approximation Made Simple. *Phys. Rev. Lett.* **1996**, *77*, 3865−3868.
(14) Anisimov, V. I.; Aryasetiawan, F.; Lichtenstein, A. I. First-Principles Calculations of the Electronic Structure and Spectra of Strongly Correlated Systems: the LDA + *U* Method. *J. Phys.: Condens. Matter* **1997**, *9*, 767−808.
(15) Ortega, Y.; Hevia, D. F. Oviedo, J.; San-Miguel, M. A. A DFT Study of the Stoichiometric and Reduced Anatase (001) Surfaces. *Appl. Surf. Sci.* **2014**, *294*, 42−48.
(16) Methfessel, M.; Paxton, A. High-Precision Sampling for Brillouin-zone Integration in Metals. *Phys. Rev. B: Condens. Matter Mater. Phys.* **1989**, *40*, 3616−3621.
(17) Wang, Z.; Sha, J.; Liu, E.; He, C.; Shi, C.; Li, J.; Zhao, N. A Large Ultrathin Anatase TiO_2 Nanosheet/Reduced Graphene Oxide Composite with Enhanced Lithium Storage Capability. *J. Mater. Chem. A* **2014**, *2*, 8893−8901.
(18) Morgan, B. J.; Watson, G. W. Role of Lithium Ordering in the LixTiO2 Anatase → Titanate Phase Transition. *J. Phys. Chem. Lett.* **2011**, *2*, 1657−1661.
(19) Monkhorst, H. J.; Pack, J. D. Special Points for Brillouin-zone Integrations. *Phys. Rev. B: Condens. Matter Mater. Phys.* **1976**, *13*, 5188−5192.
(20) Shin, J.-Y.; Samuelis, D.; Maier, J. Sustained Lithium-Storage Performance of Hierarchical, Nanoporous Anatase TiO_2 at High Rates: Emphasis on Interfacial Storage Phenomena. *Adv. Funct. Mater.* **2011**, *21*, 3464−3472.
(21) Sha, J.; Zhao, N.; Liu, E.; Shi, C.; He, C.; Li, J. In Situ Synthesis of Ultrathin 2-D TiO_2 with High Energy Facets on Graphene Oxide for Enhancing Photocatalytic Activity. *Carbon* **2014**, *68*, 352−359.

(22) Zhou, G.; Wang, D.-W.; Yin, L.-C.; Li, N.; Li, F.; Cheng, H.-M. Oxygen Bridges between NiO Nanosheets and Graphene for Improvement of Lithium Storage. *ACS Nano* **2012**, *6*, 3214−3223.
(23) Momma, K.; Izumi, F. VESTA 3 for Three-Dimensional Visualization of Crystal, Volumetric and Morphology Data. *J. Appl. Crystallogr.* **2011**, *44*, 1272−1276.
(24) Hao, B.; Yan, Y.; Wang, X.; Chen, G. Synthesis of Anatase TiO_2 Nanosheets with Enhanced Pseudocapacitive Contribution for Fast Lithium Storage. *ACS Appl. Mater. Interfaces* **2013**, *5*, 6285−6291.
(25) Augustyn, V.; Come, J.; Lowe, M. A.; Kim, J. W.; Taberna, P.-L.; Tolbert, S. H.; Abruña, H. D.; Simon, P.; Dunn, B. High-Rate Electrochemical Energy Storage through Li^+ Intercalation Psedocapacitance. *Nat. Mater.* **2013**, *12*, 518−522.